Discover Applied Sciences

Research

Investigation of debinding sintering strategy and analysis of different structure properties of printed ceramic clay materials based on liquid deposition molding technology

Shenggui Chen[1,5] · Chuang Xiao[2] · Kejiang Liu[1] · Nan Li[3] · Sadaf Bashir Khan[4] · Junchao Wu[2] · Chengdong Su[2]

Received: 16 December 2023 / Accepted: 27 February 2024
Published online: 04 March 2024

Abstract

The emergence of additive manufacturing (AM) technology for ceramic clay materials has greatly impacted the traditional pottery manufacturing industry. However, there are still limitations in post-processing and structural design for ceramic clay materials in the current field. To address these challenges, in this study, we first used orthogonal experiments to investigate the impact of the heating rate during debinding, the final sintering point, and the insulation time at the sintering point on the performance of the fabricated parts. It was further concluded that the optimal debinding sintering strategy consisted of a debinding heating rate of 0.5 °C/min, a final sintering point of 1300 °C, and a sintering point insulation time of 3 h. Under these conditions, the compressive strength of the specimens reached a maximum of 38.75 ± 4.57 MPa. Herein, we accomplished the printing of two different structures based on liquid deposition molding (LDM) technology. Through comparative analysis of the experimental results, the research solved the buckling phenomenon of flexural specimens and concluded that the octet structure exhibited superior performance. Additionally, we successfully prepared various pottery specimens, further demonstrating this study's application prospects.

Article Highlights

(1) The paper explores how to use 3D printing technology to create ceramic clay products with different shapes and structures.
(2) The paper investigates the optimal conditions for debinding and sintering processes, which affect the quality and performance of the products.
(3) The paper compares the mechanical properties and fracture mechanisms of two different internal structures, and demonstrates various applications of ceramic clay 3D printing.

Supplementary Information The online version contains supplementary material available at https://doi.org/10.1007/s42452-024-05753-0.

✉ Shenggui Chen, dgutchensg@163.com; Chuang Xiao, xiaoxcuang@163.com; Kejiang Liu, liukj@gzpyp.edu.cn; Nan Li, dglgln@163.com; Sadaf Bashir Khan, sadafbashirkhan@swust.edu.cn; Junchao Wu, 2371134201@qq.com; Chengdong Su, 1197034370@qq.com | [1]School of Art and Design, Guangzhou Panyu Polytechnic, Guangzhou 511483, China. [2]School of Mechanical Engineering, Dongguan University of Technology, Dongguan 523808, China. [3]School of Education (Normal School), Dongguan University of Technology, Dongguan 523808, China. [4]School of Manufacturing Science and Engineering, Key Laboratory of Testing Technology for Manufacturing Process, Ministry of Education, Southwest University of Science and Technology, Mianyang 621010, China. [5]Shenzhen YongChangHe Technology Co., Ltd, Shenzhen 518103, China.

Keywords Ceramic clay materials · Pottery manufacturing industry · Debinding sintering strategy · Liquid deposition molding

1 Introduction

The first thing about the traditional method of making pottery is that one must be skillful, and the softness and hardness of the ceramic clay must be well grasped; otherwise, cracks and other defects will appear in the firing of the porcelain. The second is to pull the billet; one must have skillful technique. If the force is not uniform, it will be effortless to pull the shape of bending and easy to break the billet from the bottom [1, 2]. The preparation of the billet, the degree of green body drying and the preparation of the glaze should all be considered while pulling the green body [3]. However, additive manufacturing (AM) of ceramic clay is a manufacturing method that combines ceramic clay material with AM technology. It can significantly reduce the above-complicated process, without the high handicraft requirements for blank pulling so that ordinary people can make the pottery they want [4, 5].

In recent years, ceramic clay AM has been fully developed through technological exploration and innovation [6–8]. However, the ceramic clay has unique properties and process requirements, combining it with AM technology is challenging [9, 10]. The earliest research into ceramic clay AM dates back to 2005 when Dr. Behrokh Khoshnevis invented a technique called Contour Craftings, which focuses on creating smooth and accurate flat or free-form surfaces by extruding the material using computer control. It is expected to be used to construct entire large buildings in one piece using various building materials such as ceramic clay, plaster and concrete [11]. However, it wasn't until 2015, when Dutch design studio DUS Architects built a large-scale mobile printer called the "KamerMaker" in Amsterdam, that ceramic clay AM began to attract wider attention. It can print a variety of sized ceramic forms, marking the beginnings of ceramic clay AM [12]. In the following years, researchers have explored using different ceramic clay raw materials, improved printer design and control systems, and optimizing printing parameters to enhance print quality and efficiency [13–15]. In 2023, designer Simon Pavy, in collaboration with global design agency Entreautre, used a special 3D printer designed by renowned Dutch artist Olivier Van Herpt that is specialized in ceramic clay printing and is capable of extruding ceramic clay layer by layer to form filaments. A 3D-printed cooler has been successfully developed that promises to revolutionize cooling methods [16]. In addition, the raw material chosen for this type of printing is inexpensive ceramic clay, which is significantly less expensive than metal, and the printer does not require as high technical requirements as those for metal molding [17–19]. Metal or resin molding requirements for preserving liquid raw materials or liquefaction are very high for the printer's technical requirements [20]. However, ceramic clay AM equipment for storing ceramic clay is simple, only stored in a rigid plastic tube. This ceramic clay has plasticity, high-temperature resistance, environmental sustainability, rich texture, and other characteristics [20–22]. As the technology progresses continuously, ceramic clay AM applications are gradually expanding.

Although ceramic clay AM technology has made good progress in pottery manufacturing industry [23, 24], there are still some drawbacks and challenges to overcome: (1) Post-processing requirements: The current field of inquiry into the ceramic clay debinding and sintering process lacks quantitative analysis and may significantly impact the final product's quality. (2) Structural design: The structural design of ceramic clay AM is also a challenge. Due to its characteristics, some complex structures and details may be difficult to realize. Also, the design needs to consider the limits of the material and its possible shrinkage and deformation during the printing process. As a result, to explore the best post-treatment method, this research first used a three-factor, three-level orthogonal experiment to examine the effects of the debinding heating rate, the final sintering point, and the sintering point insulation time on the performance of fabricated parts. Besides, a thick glass slide as a carrier can greatly reduces the deformation and warping caused by shrinkage during the drying process of ceramic clay. Then, under optimal process parameters, two different structures were used for molding and manufacturing compression-resistant parts, and the performance differences were analyzed based on digital image correlation (DIC) technology.

Table 1 Properties of cerami clay materials

Characteristic	Proportion	Moisture content	Viscosity	Temperature	Shrinkage	Strength
Value	2.6	18	0.8	1200–1400	10–15	15–40
Unit	g/cm^3	%	Pa·s	℃	%	MPa

Table 2 LDM technical parameters

Software printing parameters	
Nozzle size (mm)	0.8
Layer height (mm)	0.6
Wall thickness (mm)	0.8
Infill density (%)	40
Flow rate (%)	80
Infill speed (mm/s)	40
Wall speed (mm/s)	20
Retraction distance (mm)	0.625
Equipment printing parameters	
Thrust extrusion ratio	0.7
Extrusion rate (%)	100
Extrusion capacity (%)	100

2 Materials and methods

In this research, we used MOORE 1 ceramic clay 3D PRINTER equipment and LOBO evacuated 20 KG bags of ceramic clay consumables for the printing, both purchased from Aidijia Additive Digital Technology (Guangzhou) Co., Ltd. ceramic clay is one of the richest and most traditional materials in the world. The main properties of the ceramic clay material are shown in the Table 1. Its defining mechanical properties are its plasticity when wet and its ability to harden when dry or fired. Ceramic clay has a wide range of water content, from the minimum water content at which the ceramic clay is just wet enough to be molded (known as the plastic limit) to the maximum water content at which the molded ceramic clay is just dry enough to retain its shape (also known as the liquid limit) [7]. The ceramic clay composition consists mainly of ceramic clay minerals and water. The fine particles in ceramic clay minerals have a negative charge that allows them to adsorb water molecules and form a gelatinous substance. When the ceramic clay is subjected to external forces, the internal ions interconnect and adhere. The resulting wet-state adhesion imparts cohesion to the ceramic clay, making it plastic [8].

2.1 LDM process manufacturing

Specific process manufacturing first uses computer-aided software to design the required model and convert it into STL format imported into the printing equipment adapted software Ultimaker Cura for slicing. The selection of parameters such as nozzle size, printing layer thickness, and filling density in the experiment was made after comparing printing tests of several groups of experiments, and the final preferred results are shown in Table 2. In the experiment, the material needs to be pre-treated first. The obtained bagged ceramic clay consumables are mixed with a small amount of water solution to improve the wettability of the material, which is mixed well and placed in the cylinder by vacuuming in the ceramic clay refining machine (Jingdezhen City Longfu Ceramics Equipment Factory, China) to avoid the presence of large bubbles that make the printing process intermittent. The subsequent structure fabrication included selecting a gradient model, including octet and cubic forms, which were systematically stacked layer by layer to generate the intended three-dimensional prototype. After printing, the prototypes were removed

and placed in the laboratory at room temperature (25 °C) for 1 day (it should be noted that the flexural specimens are best placed on thick slides to help avoid bottom warping of the prototypes during natural air drying). Finally, the fabricated parts will be placed in the heat treatment furnace (SXL-1800C, Shanghai Jujing Precision Instrument Manufacturing Co., Ltd.) for debinding and sintering to complete the specimen preparation; the process is shown in Fig. 1. The composition of the original clay material was also tested for XRD characterization in the figure, which further argues that its main components are quartzite, kaolinite, mullite and other minerals.

2.2 Characterization

An X-ray diffractometer (XRD: Smart Lab, Rigaku, Japan) 2θ was used at 6 kV from 10° to 80° with a scanning rate of 2°/min to analyze the main components of the ceramic clay materials. Thermogravimetric (TG), derivative thermogravimetric (DTG) and differential scanning calorimetry (DSC) analysis were performed using an STA 2500 instrument (Netzsch, Germany) in the air at a heating rate of 10 °C/min (from 30 to 1500 °C), followed by determinations of the rate of debinding sintering and insulation time. Flexural and compression tests were performed on a computer-controlled electronic universal testing machine (LD23.104, LSI, China)according to ASTM C1424-15 and ASTM C1161-18. VIC-2D 6-2D analysis software and VIC-3D 9-3D analysis software were used for data integration during the DIC testing process, equipped with VIC-Snap-8, VIC-Snap-9 acquisition software, and the camera model of the final captured image was Grasshopper 3 GS3-U3-91S6M.

2.3 Experimental design of Taguchi's method

Previous research has shown that three factors in the post-treatment process, namely, the debinding heating rate, the final sintering point, and the sintering point insulation time, have a significant effect on the properties of the fabricated parts, such as microstructure, dimensional shrinkage, relative density, and flexural strength [25, 26]. The orthogonal experiments conducted by the Taguchi method were used to comprehensively analyze these three factors to determine the degree of their influence and optimize the post-processing conditions. So that the optimal debinding and sintering parameters could be selected by comparing the differences in the final properties of the specimens. Moreover, orthogonal experimental design is an efficient, accurate, statistically reliable, economical and practical multi-factor experimental design method. It can help researchers systematically explore the influence of multiple factors on the results, optimize the experimental scheme, and improve the research efficiency and credibility of the results [27–29]. It has been widely used in optimizing material configurations and process parameters. The three factors selected in this research are listed in Table 3, and for ease of reference, the influencing factors, data variables, and experimental numbers are abbreviated as F, V, and N. The design of orthogonal experiments is listed in Table 4.

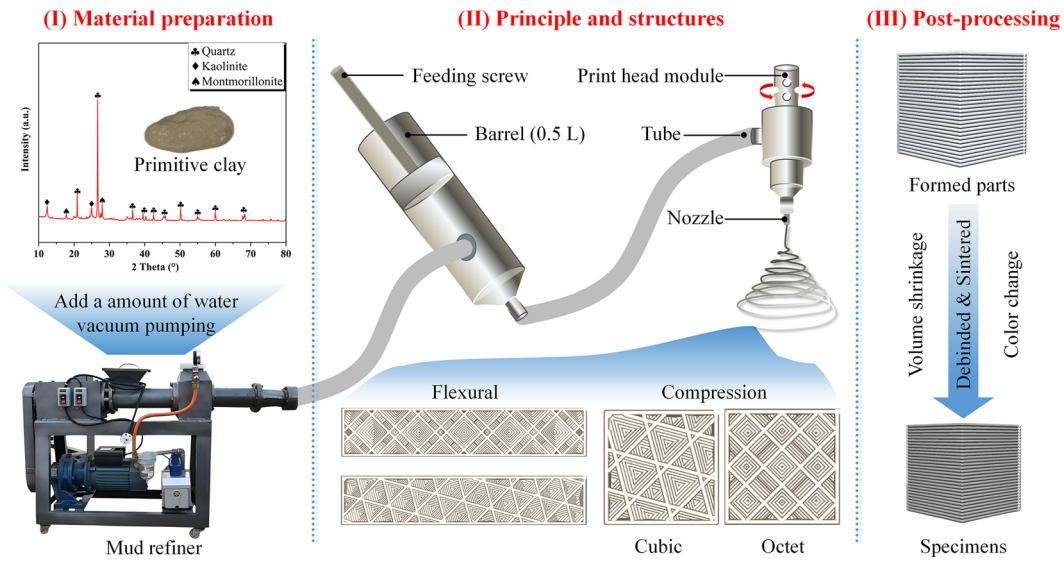

Fig. 1 Molding and printing process of ceramic clay material

Table 3 Influencing factors, numerical variables, and corresponding values of heat treatment orthogonal tests

Factors		Variable		
		V1	V2	V3
F1	Debinding heating rate (°C/min)	0.5	1.5	2.5
F2	Sintering endpoint (°C)	1200	1300	1400
F3	Endpoint insulation time (h)	1	3	5

Table 4 L9 (3^4) arrays performing orthogonal experiments

Number	Factors		
	F1 (°C/min)	F2 (°C)	F3 (h)
N1	0.5	1200	1
N2	0.5	1300	3
N3	0.5	1400	5
N4	1.5	1200	3
N5	1.5	1300	5
N6	1.5	1400	1
N7	2.5	1200	5
N8	2.5	1300	1
N9	2.5	1400	3

3 Results and discussions

3.1 Heat treatment process analysis

Debinding sintering is a standard post-treatment process for manufacturing and processing ceramic clay materials. It can be controlled by the sintering temperature and time to make the organic material in the ceramic clay burn out; the organic content in the ceramic clay will be significantly reduced, effectively changing the chemical composition of the ceramic clay. This is very important for some need to adjust the composition of the specific ceramic clay materials. Therefore, adequate material testing and process optimization are required before using the debinding sintering process to ensure that the desired results are achieved.

3.1.1 Analysis of the degreasing and sintering process

The results of the TG test are shown in Fig. 2a. In order to better analyze the thermal stability and thermal decomposition mechanism of the samples, we plotted the DTG curves. From the figure, it can be seen that when the test temperature was increased from room temperature to 200 °C, part of the specimens' mass was lost, mainly due to the loss of the unvolatilized aqueous solution during the conservation period [30–33]. Since 200 °C, the exothermic rate began to become larger, indicating that a small amount of organic substances (organic gelling agents, plasticizers, etc.) in the ceramic clay started to undergo thermal decomposition, releasing gases and leaving solid residues. This resulted in a slight mass loss, but the quality of the ceramic clay remained basically stable. Based on the DTG curve, it can be seen that a significant mass change occurs in the process from 40 to 800 ℃, which is mainly due to the accumulation of carbon and organic matter under high temperature conditions and the reaction of oxygen into carbon dioxide and other gases volatilized, resulting in the loss of mass. Besides, some amorphous compounds in the ceramic clay will also be transformed into crystal structures, further aggravating the quality loss. From 800 to 1500 °C, the quality of the specimens did not decrease but increased. On the one hand, it shows that the organic matter in the specimens is almost completely removed after 800 °C; on the other hand, it is mainly due to the reaction of silica, alumina, iron oxide, and other compounds with oxygen that makes the quality increase, so the debinding temperature is set at 800 °C. In addition, the process of exothermic reaction continued to appear in the small band of peaks, mainly in the specimen of some inorganic materials that also gradually occurred in the crystal phase change (including quartz,

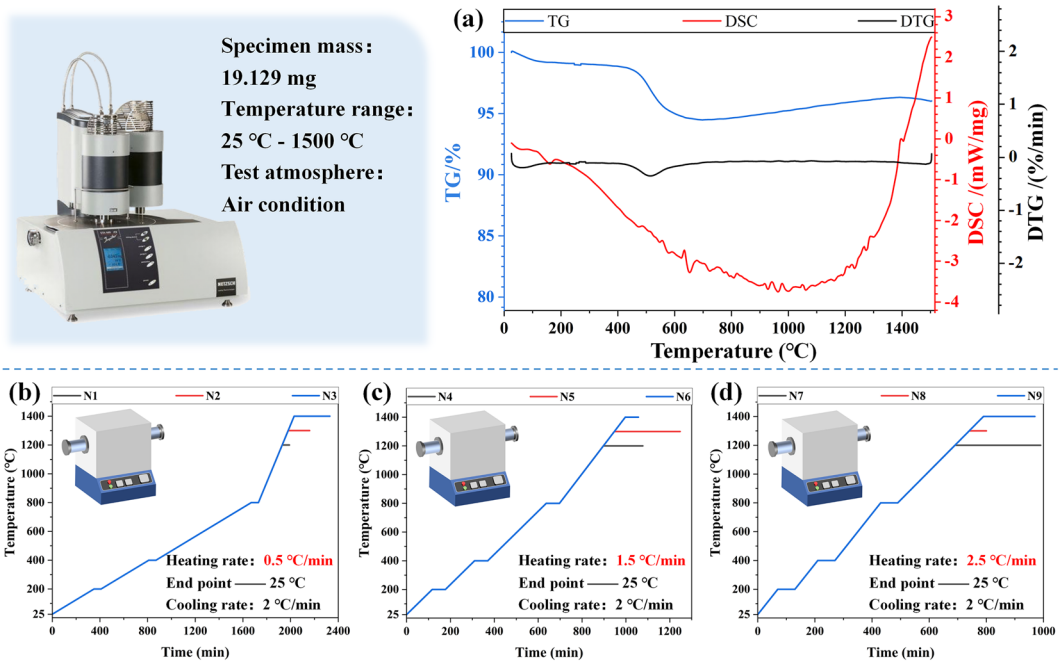

Fig. 2 **a** TG-DSC curve. Debinding sintering curve of **b** N1–N3, **c** N4–N6, **d** N7–N9

feldspar, mica, and other minerals crystallization); these inorganic materials at high temperatures will rearrange and aggregation lead to the disintegration of the original crystalline structure, the formation of ceramic clay materials of dense structure. Since the beginning of 1200 °C, the end of the thermal liberation of organic matter heat, grains began to form. The exothermic effect is dramatically transformed to the heat-absorbing effect, and the transformation of the crystalline phase is basically completed at 1300 °C. Some components of the ceramic clay (such as silicates, carbonates, etc.) will melt into a liquid at this stage, which combines with other unmelted particles to form a viscous molten mixed object that aids in the bonding of the ceramic clay particles to each other. The presence of the liquid phase can fill the voids between the ceramic clay particles, increasing the contact area between the particles and thus increasing the bonding strength between the particles. Besides, it can make the ceramic composition uniformly distributed, avoiding the weaknesses and defects caused by the inhomogeneity of the composition, thus improving the strength of the ceramics. After 1300 °C, the curve tends to increase in a straight line and no longer fluctuates, mainly heat-absorbing reactions. It is deduced that the cause of its production is the formation of a significant number of liquid phases in the mud and the growth of the grains. Although the ceramic clay material will experience varying degrees of volume contraction during the debinding and sintering processes, the final mass and the initial mass change are less than 5%. This means that the post-treatment of ceramic clay specimens after the densification of a significant increase relative to other materials greatly enhances its mechanical properties.

The results of TG and DSC have analyzed the various changes that may occur during the post-treatment process of ceramic clay green body; however, the parameter settings for the actual debinding and sintering curves are still insufficient. To obtain the best-sintered parts, this research is based on the above analysis results; for the debinding process of the heating rate, the final sintering point and the final holding time for a comprehensive analysis, F1 was set to 0.5, 1.5, 2.5 °C/min, F2 was set to 1200, 1300, 1400 °C, and F3 was set to 1, 3, 5 h. Then screened out the optimal debinding sintering conditions through orthogonal experiments for comparison. The optimal debinding sintering conditions, the specific process, is shown in Fig. 2b–d (cooling process rate is 2 °C/min, no longer displayed).

3.1.2 Comparative analysis of compressive strength of sintered parts under different conditions

Compressive strength is one of the most important indicators of the mechanical properties of ceramic clay materials, which is of great value for product quality, structural stability, processing performance and application areas. In this research, we first designed cylindrical specimens with a diameter of 15 mm and a height of 20 mm, printed a cumulative total of 50 specimens (with no less than three in each group) and post-treated the specimens according to different

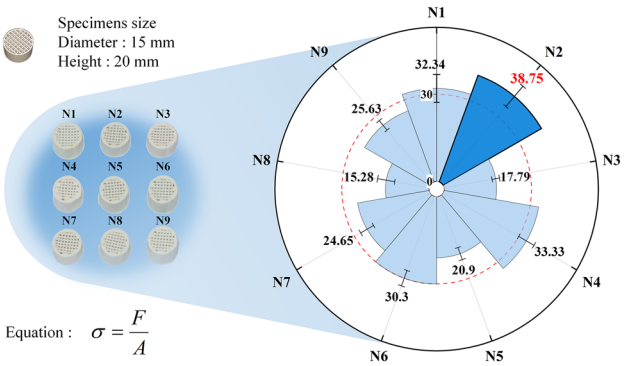

Fig. 3 Compressive strength property analysis

Table 5 Analysis of each factor's range and degree of influence on the compressive strength of fabricated parts

Factors	V1	V2	V3	Range
F1	29.40	28.18	21.86	7.54
F2	29.88	24.98	24.57	5.31
F3	25.75	32.57	21.11	11.46

debinding and sintering conditions. Then, the specimens were subjected to compressive tests in batches to compare the performance differences for optimizing post-treatment conditions. The specific experimental results are as follows: the optimum performance was achieved at a debinding heating rate of 0.5 °C/min, a sintering point of 1300 °C, and a insulation time of 3 h, reaching 38.75 ± 4.57 MPa, as shown in Fig. 3.

Based on the compressive strength obtained for each condition a comprehensive analysis was carried out to investigate the degree of influence of F1, F2 and F3 on the fabricated parts. Table 5 shows the degree of influence of the three factors on the compressive strength of the sintered parts based on the analysis of extreme deviation of orthogonal tests. Obviously, the holding time at the final point has a significant influence on the sintered parts. The length of the holding time will directly affect the sintering degree of ceramic clay material and the degree of perfection of grain growth. To obtain a uniform and dense structure and improve the compressive strength, the holding time needs to be determined according to the specific ceramic clay material and the requirements of the fabricated parts. If the holding time is too short, the sintering is incomplete, the grain growth is insufficient, and the minerals and organic substances in the ceramic clay material may not react sufficiently and decompose. This will lead to the existence of voids and defects inside the fabricated parts, and the compressive strength will be affected, which is similar to the heat preservation of 1 h in this research. However, the holding time of 5 h may be too long, resulting in excessive sintering. This will make the grain growth too large [34, 35], the grains in the ceramic clay material will be too large, and the internal structure of the fabricated parts will become inhomogeneous, prone to cracks and deformation. It may make the final sintered parts brittle to a certain extent. At the same time, too much liquid phase may be formed, resulting in excessive sintering contraction of ceramics or even causing sintering failure, which reduces the compressive strength.

Therefore, to obtain the high compressive strength of fabricated parts, it is necessary to control the holding time at the final sintering point of the ceramic ceramic clay material. So that it can complete the process of sintering and grain growth within an appropriate time, thus obtaining a uniform and dense structure and improving the compressive strength.

Shrinkage has an important value for ceramic ceramic clay fabricated parts. ceramic clay shrinks during drying and sintering, and shrinkage is a measure of the degree of deformation of the ceramic clay material, which has an essential influence on the dimensional stability and quality control of fabricated parts. Shrinkage can be used to control the size of manufactured parts [36, 37]. By knowing the shrinkage rate, researchers can take appropriate measures to prevent these defects from occurring and improve the quality of manufactured parts. Therefore, the shrinkage of ceramic clay materials must be considered and controlled in the design of material development and molding process to ensure stable processing and quality fabricated parts.

Shrinkage value for ceramic clay fabricated parts is reflected in dimensional control, quality control and material stability, and better performance and quality of fabricated parts can be obtained by controlling and optimizing shrinkage. In this research, the comparative analysis of the shrinkage test was carried out for specimens under nine debinding sintering conditions, and the specific results are shown in Table 6. According to the previous studies, the shrinkage in X and Y

Table 6 Shrinkage in XY and Z directions in nine sets of tests N1-N9

Shrinkage (%)	N1	N2	N3	N4	N5	N6	N7	N8	N9
XY	14.07	15.47	11.53	14.60	13.00	13.60	13.53	13.67	12.27
Z	16.78	20.11	14.00	18.83	18.61	16.83	18.28	19.61	15.72

directions are similar and the shrinkage in Z direction will be greater than the shrinkage in XY direction [38–40], which is consistent with this research. This research concludes that the final sintering point has the greatest influence on the shrinkage of fabricated parts. The specific results are shown in Fig. 4. This is because the sintering temperature directly affects the structure and physical properties of the ceramic clay, which produces different results for the sintering process, structure formation, crystal phase transformation and grain growth. Higher sintering temperatures induce the particles in the ceramic clay to bond more tightly and form a more stable structure, which leads to significant shrinkage. Conversely, lower sintering temperatures may result in less stable structures and less shrinkage. Therefore, choosing the appropriate sintering temperature can achieve a balance between the structure, densification, crystal phase transition and grain growth of the ceramic clay, and also control the products' shrinkage to ensure the products' quality and performance.

3.2 Influence of structural differences on the performance of fabricated parts

The internal structure of the ceramic clay fabricating parts has an important impact on its performance. Through the optimization of the structural design, you can control the distribution and size of pores in the printed ceramic clay specimens and a variety of different sizes and shapes of pores, which have a direct impact on the material's water absorption, permeability, sintering properties and mechanical properties, etc. So as to improve the densification of the fabricated parts and increase the Strength and wear resistance [41]. Besides, the use of hollow structures or skeleton structures in the structural design can reduce the weight of the fabricated parts and improve the strength and stiffness of the fabricated parts. For example, in the design of ceramic filters, reasonable structural design can be used to increase the filtration efficiency and fluid flux [42, 43]. It is important to note that the effects of these internal structures are interrelated, and the properties of ceramic clay materials can be improved and adjusted by adjusting and controlling the internal structures. Therefore, understanding and optimizing internal structures are very important in developing and preparing ceramic clay materials.

3.2.1 Analysis and solution of the warping phenomenon of ceramic clay material bending specimens

When printing ceramic clay, the existence of specimen warping phenomenon will lead to product shape irregularity, affecting the appearance of the product aesthetics. This will lead to a decline in the stability of the product in the use of the process, especially for the need for stacking or assembly of the product; the warping will affect the product's connecting and fixing effect. Moreover, if the ceramic clay specimen warps seriously, the size and shape of the product deviate from the design requirements, resulting in poor processing accuracy, thus affecting the assembly and use of the product.

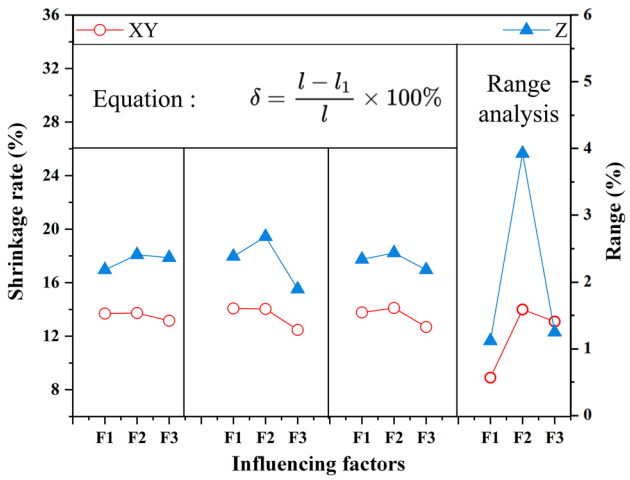

Fig. 4 The influence degree and range of three factors on XY direction and Z direction of molded parts

In this research, a more obvious warping phenomenon occurred when the drying and conservation treatment of both structures was carried out. In order to reduce the warping problem of the ceramic clay prints, the experiment was carried out using an octet gradient structure for comparative analysis under four conditions with the same conservation time. Two kinds of carriers were used on the carrier substrate: Fluorinated ethylene propylene (FEP) release film and 7105 thick glass slide, and the attachment type of the printing platform on the process was set to none (no platform attachment type) and raft (full to the edge), and the experimental results are shown in Fig. 5. The first case carrier is a FEP release film without any type of platform connection, and after 12 h of natural drying, an evident unrecoverable warping phenomenon emerged, as illustrated in Fig. 5a. The warping issue was somewhat reduced in the second instance by using the same FEP release film and switching the platform attachment type to full to the edge, as illustrated in Fig. 5b. In the third case, when the FEP release film was replaced with a thick slide and no platform attachment type, it can be seen that there is basically no obvious warping phenomenon, as shown in Fig. 5c. In the fourth case, using thick slides and full-to-edge platform attachment type, on the contrary, there is a slight warping phenomenon in the place where the specimen meets the edge, as shown in Fig. 5d.

Comprehensive analysis of the above phenomenon, the use of FEP release film, ceramic clay specimens in the drying process will produce upward capillary force. This is because the moisture in the ceramic clay specimen gradually evaporates during the drying process, resulting in air infiltration into the inside of the ceramic clay specimen, forming a negative pressure. According to the principle of capillary phenomenon, the negative pressure causes the moisture inside the ceramic clay specimen to move upward, generating an upward capillary force [4, 44]. This upward capillary force helps to promote the rapid evaporation of water inside the ceramic clay specimen and accelerates the drying speed. However, due to the thinness of the FEP release film, the downward adsorption force on the specimen is not enough to counteract the upward capillary force of the ceramic clay drying, resulting in the release of the film, which leads to noticeable warping. When the platform attachment type full to the edge was added, the presence of the attached ceramic clay material would increase its gravity during the warping process at both ends of the specimen, further counteracting part of the upward capillary force and allowing the warping phenomenon to be alleviated. When the carrier is made of thick slides, a strong adsorption force is generated between the specimen and the slides, which is greater than or equal to the upward capillary force during the ceramic clay drying process, avoiding the warping phenomenon. After the addition of the platform attachment type, the slide also generated a strong adhesion to the ceramic clay around the specimen. The specimen was subjected to upward capillary force different from that generated by the surrounding attached ceramic clay, which resulted in the interface between the specimen and the surrounding attached ceramic clay became unusually fragile. At a certain limit time, sudden tensile breakage occurs, and the instantaneous upward capillary force exceeds the downward adsorption force of the slide, resulting in a slight warping phenomenon at both ends of the specimen. Based on the above analysis, thick slides were chosen as the carrier, and the platform attachment type of none was sufficient. In addition, this research also tested the extreme case, choosing the optimal conditions based on another slide on the top of the specimen to reduce the possible warping phenomenon further. However, the experimental results showed that this solution greatly reduced the drying rate of the ceramic clay specimens, and even after removing the top slide after

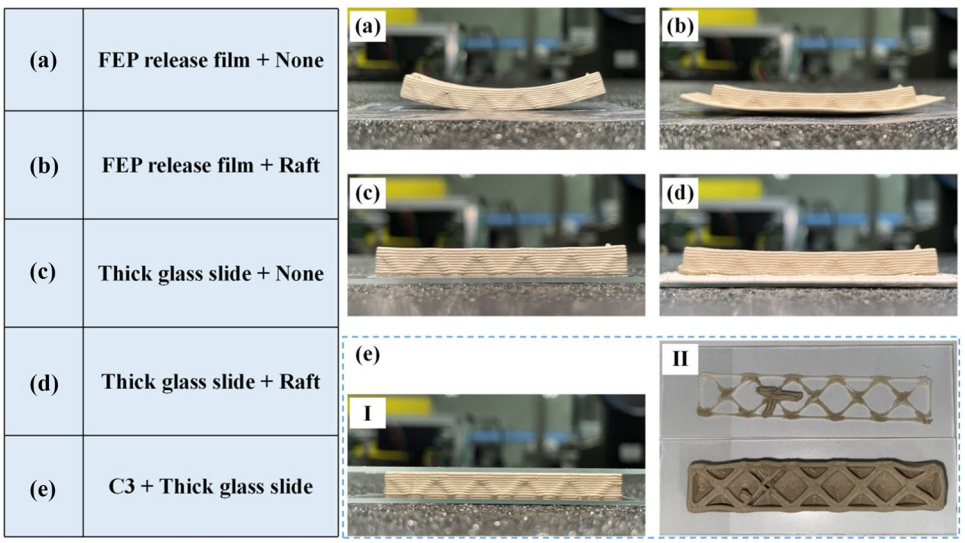

Fig. 5 Warping of ceramic clay flexural specimens under different conditions

12 h of drying, it was still not completely dried. Partdried of the ceramic clay became stuck to the top slide, compromising the integrity of the original specimens, as illustrated in Fig. 5e.

Through the comprehensive consideration of the above factors, in order to effectively reduce the pottery ceramic clay prints appear warping problem, and get a better printing effect, it is best to choose the thick system slides as the carrier, the platform attachment type selection of none. (However, it must be noted that, if you want to carry out some large-scale planar model or solid model printing, you still need to choose FEP release film or similar cling film as a carrier. Otherwise, it may be due to the uneven adsorption and capillary force between the slide and the specimen at different locations, resulting in different degrees of cracking in the articulated part of the specimen, which ultimately makes the model damaged).

3.2.2 Comparative analysis of flexural and compressive properties of two structures

Based on the above optimal conditions of the debinding sintering process and solving the warping phenomenon of the flexural specimens, the printing of the two structures was then carried out. The dimensions of the flexural specimen were 60 mm * 12 mm * 6 mm in length, width and height, and the dimensions of the compressive specimen were 18 mm cubes [45]. The compressive and flexural tests performed on the ceramic clay specimens evaluated the mechanical properties of the two internal structures to determine their load-bearing capacity and durability in real-world applications. These tests can help determine the ceramic clay specimens' strength, stiffness, and deformation capacity so that appropriate materials and structures can be selected for the design and manufacture of ceramic products. Through these tests, the performance of ceramic clay specimens when subjected to pressure and bending forces can be evaluated to ensure the quality and reliability of the product, and ultimately the performance differences between the two structures can be further comparatively analyzed. This research concludes from the experimental comparisons that the octet's internal gradient structure will outperform the cubic's internal gradient structure in terms of both compressive (in both directions) and flexural strengths. It ultimately achieves compressive strengths of 23.25 ± 2.10 MPa and 9.25 ± 0.44 MPa in both directions and flexural strength of 13.94 ± 1.32 MPa. While the cubic structure gains compressive strengths of 14.90 ± 2.41 MPa and 8.90 ± 1.44 MPa in both directions and flexural strength of 12.74 ± 0.84 MPa, the specific results are shown in Fig. 6.

3.2.3 Fracture mechanism analysis of two structures

When ceramic clay specimens fracture during compressive testing, analysis of the fracture mechanism can help determine the root cause of the problem, which is important for failure analysis and problem-solving. The study can identify the factors that led to the fracture, such as the material composition ratio, preparation process or sintering temperature, which in turn can guide the optimization of the production process to improve the compressive properties and stability of the material. Digital Image Correlation (DIC) technology is a non-contact measurement technique that enables the analysis of images to obtain measurements without the need for physical contact with the surface of the material. In addition, it provides highly accurate displacement and deformation measurements, which is important for studies that require accurate measurement of small deformation or fine structure of ceramic clay materials [46, 47].

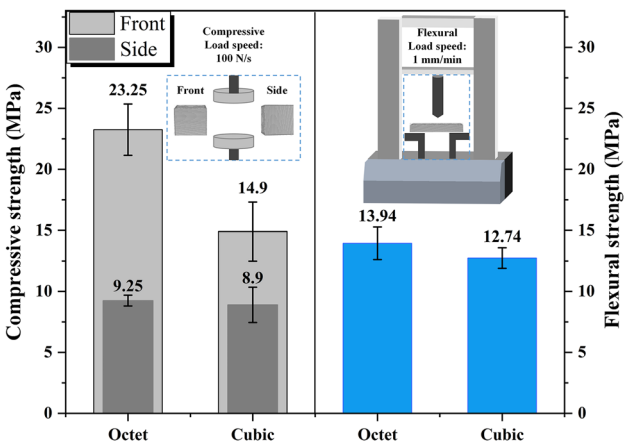

Fig. 6 Mechanical properties testing of two different structures

In this research, a qualitative analysis of the fracture mechanism and the stress analysis of the two ceramic clay structures is needed to investigate the key areas where the two ultimately show differences in compressive strength. The first step is to use DIC to help research the damage behavior of the ceramic clay materials. Observing the images before and after the damage can analyze the damage pattern and mechanism. Then the mechanical properties and deformation behavior of the material can be studied. As seen in Fig. 7, from the beginning of the crack appearance to the crack propagation before final breakage, it is evident that the fracture mechanism of both structures in both directions is compression brittle fracture triggered by crack extension. Also, as shown by the proof documents Video S1–S4, shear damage and compression damage occur throughout the whole compression process. However, the difference is that the octagonal structure in the fracture process first appeared as a crack, and then, along with the continuous addition of stress, will be subjected to stress dispersion and then gradually appeared more than one obvious crack, began to occur fracture. The damage of the octet structure along the internal structure articulation site is prone to produce stress concentration in the place where the regular fracture of the large section occurs, as shown in Fig. 7a, c.

On the other hand, the instability of the internal structure during the application of force is what causes the fracture of the cubic structure in both directions, leading to the abrupt emergence of many fractures. The ultimate fracture is similar to the crushed, as illustrated in Fig. 7b, d. As a result of the cracks' growth during the cross-union process, which caused the interior structure collapses due to secondary stress concentration. In summary, although the same fracture is caused by crack extension, the process of crack emergence in the octet is much more regular, and the pre-cracks basically do not cross each other. However, the emergence of cracks in the cubic structure tends to be unorganized, and the cracks tend to cross each other from the time they appear, which will exacerbate the degree of structural damage. Moreover, after testing, the octet structure of the ceramic clay specimen is more stable than the cubic structure, so the octagonal structure has better performance in both front and side. In addition, whether it is an octet or cubic structure, the corresponding forward compression performance is significantly better than its lateral compression. On the one hand, the reason comes from the specimen in the manufacturing process and degreasing and sintering process in the Z direction of the interlayer bonding better tight, which will make in the compression test process in the forward compression performance is significantly better than the side of the compression performance. On the other hand, due to the XY direction and the Z direction, the contraction rate is different, which means that the compression of its ability to withstand the force of the area is smaller. This can further exacerbate the generation of lateral compression process of rupture.

3.3 Demonstration of fabricated parts

The effective preparation of numerous specimen parts without the need for support was achieved by the use of the LDM printing technique, as seen in Fig. 8a shows the various parts of the Lupin lock and can be articulated after debinding and sintering. Figure 8b, c shows the model fabrication of two different types of vases, and Fig. 8d, e shows a two-dimensional flat model of a teacup coaster as well as the tip portion of a spatula, respectively. Overall, ceramic clay molding has been gradually replacing traditional pottery manufacturing, making it easier to make pottery and also helping to promote quality and innovation in artwork.

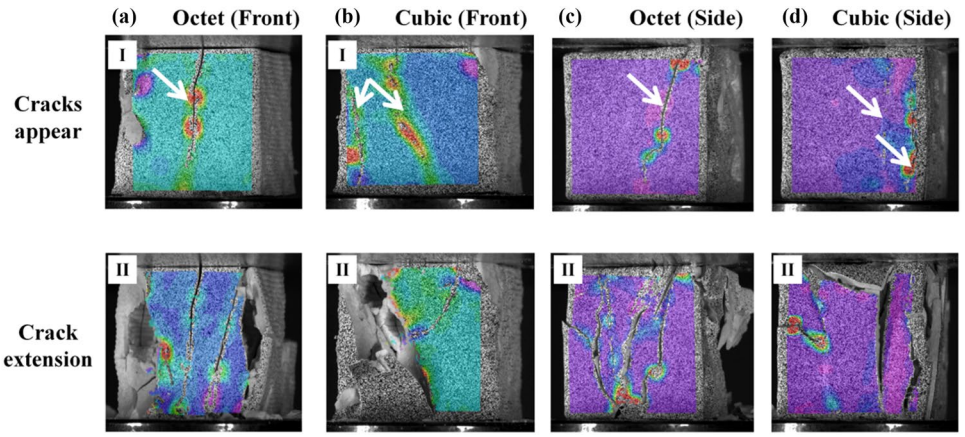

Fig. 7 Fracture of two structures in two directions. **a** Octet (Front). **b** Cubic (Front). **c** Octet (Side). **d** Cubic (Side)

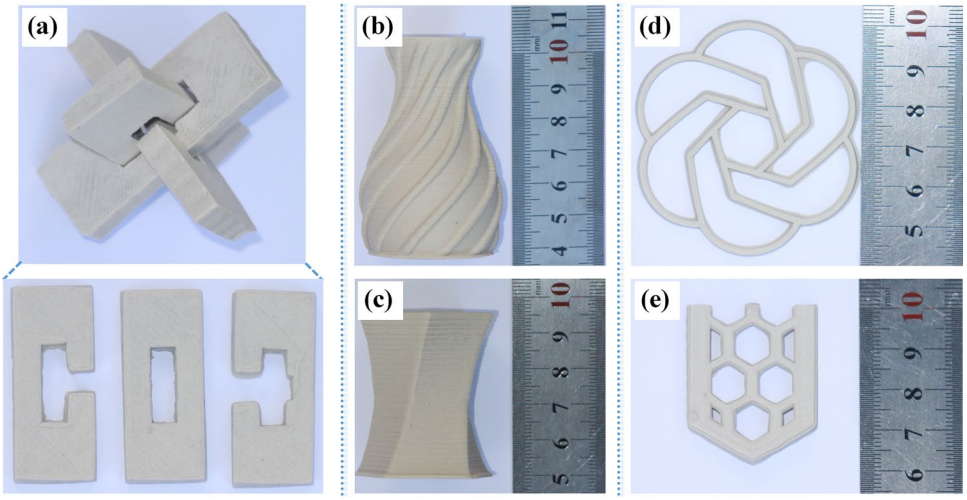

Fig. 8 Demonstration parts of sintered ceramic clay manufactured using LDM technology. **a** Lupin lock. **b**, **c** Vase. **d**, **e** Two-dimensional flat model

4 Conclusions

This study involved the utilization of LDM technology to mold ceramic clay materials. Subsequently, three pertinent factors affecting the post-processing of ceramic clay materials were thoroughly examined by analyzing TG data in conjunction with the results of an orthogonal test performance. The aim was to ascertain the extent of influence exerted by each factor and establish suitable parameters for the debinding and sintering processes. Further, two different structures were selected for molding and manufacturing; the analysis process solved the phenomenon of bending specimens that are prone to warping. Then the structure was preferred by the compressive strength test results, and then the DIC test was used to analyze the fracture mechanism of the different structures. Finally, this research was also successful in printing a variety of models. The following are the conclusions of this research:

(1) The compressive strength results of the orthogonal tests of the ceramic ceramic clay specimens in the research showed that the best performance was achieved when the debinding temperature increase rate was 0.5 °C/min, the final sintering point was 1300 °C, and the insulation at the sintering point was 3 h. The compressive strength reached 38.75 ± 4.57 MPa
(2) Based on the extreme difference analysis method of the orthogonal test, it is concluded that in the post-treatment process, the holding time at the sintering point has a significant influence on the mechanical properties of the fabricated parts. In contrast, the sintering point has the greatest impact on the shrinkage rate of the manufactured printed parts.
(3) In the research, a thick glass plate was used as a carrier to better solve the phenomenon of easy warping of flexural specimens, and the causes of distortion were analyzed by comparing the adsorption force generated by the substrate with the capillary force generated by the volatilization of the specimen material.
(4) According to the mechanical property test results of the two different structures, the performance of the octet structure is remarkable, and its flexural strength and compressive strength (in both directions) reach 13.94 ± 1.32 MPa and 23.25 ± 2.1 MPa (front), 9.25 ± 0.44 MPa (side), respectively.
(5) The fracture mechanisms of the two structures were qualitatively analyzed based on DIC tests, and compression damage, shear damage, and compression crushing occurred. However, due to the structural instability of the cubic structure in the process of compression, stress concentration is prone to occur, resulting in the premature emergence of crack extension cross and structural failure.
(6) Finally, this research successfully printed models of combinable Lupin lock sub-parts, three-dimensional vases, and two-dimensional planar specimens, verifying this printing technology's feasibility in various fields.

Acknowledgements This research is financially supported by the Key scientific research platforms and projects of Guangdong universities (2023WCXTD035 and 2022ZDZX3064 and 2023ZDZX4114 and 2023ZDZX3072 and 2023KCXTD071), the research project of Guangzhou Panyu Polytechnic (2023KJ04), the research platform of Guangzhou Panyu Polytechnic (2022KYPT03), the Guangzhou higher education teaching

quality and teaching reform project (2022JSJXCXTD005 and 2022CXCYJH002). the Dongguan University of Technology Students Innovation and Entrepreneurship Training Program Projects (202211819038).

Author contributions SC: conceptualization, methodology, investigation, formal analysis, visualization, writing—original draft, funding acquisition; CX: methodology, validation, data curation, writing—original draft; KL: investigation, formal analysis, supervision; NL: methodology, resources, supervision; sbk: investigation, validation, formal analysis; JW: visualization, investigation; CS: investigation; formal analysis.

Funding This study was funded by the Key scientific research platforms and projects of Guangdong universities, 2023WCXTD035 and 2022ZDZX3064 and 2023ZDZX4114 and 2023ZDZX3072 and 2023KCXTD071, the research project of Guangzhou Panyu Polytechnic, 2023KJ04, the research platform of Guangzhou Panyu Polytechnic, 2022KYPT03, the Guangzhou higher education teaching quality and teaching reform project, 2022JSJXCXTD005 and 2022CXCYJH002, the Dongguan University of Technology Students Innovation and Entrepreneurship Training Program Projects, 202211819038.

Data availability No datasets were generated or analysed during the current study.

Declarations

Competing interests The authors declare that the data supporting the findings of this study are available within the paper and its Supplementary Information files.

References

1. Tsetlin YB. The origin of ancient pottery production. J Hist Archaeol Anthropol Sci. 2018;3(2):193–8. https://doi.org/10.15406/jhaas.2018.03.00083.
2. Bolaji KI, Samuel SA. Adaptation prospects of traditional pottery practice in contemporary Erusu Akoko. Int J Hum Soc Sci Insights Transform. 2017;3(2).
3. Ngo TD, Kashani A, Imbalzano G, Nguyen KTQ, Hui D. Additive manufacturing (3D printing): a review of materials, methods, applications and challenges. Compos B Eng. 2018;143:172–96. https://doi.org/10.1016/j.compositesb.2018.02.012.
4. Ruscitti A, Tapia C, Rendtorff NM. A review on additive manufacturing of ceramic materials based on extrusion processes of clay pastes. Cerâmica. 2020;66(380):354–66. https://doi.org/10.1590/0366-69132020663802918.
5. Şahin HG, Mardani-Aghabaglou A. Assessment of materials, design parameters and some properties of 3D printing concrete mixtures; a state-of-the-art review. Constr Build Mater. 2022. https://doi.org/10.1016/j.conbuildmat.2021.125865.
6. Abdallah YK, Estévez AT. 3D-printed biodigital clay bricks. Biomimetics. 2021. https://doi.org/10.3390/biomimetics6040059.
7. Bergaya F, Lagaly G. General introduction: clays, clay minerals, and clay science. Dev Clay Sci. 2006;1:1–18. https://doi.org/10.1016/B978-0-08-098258-8.00001-8.
8. Moreno-Maroto JM, Alonso-Azcárate J. What is clay? A new definition of "clay" based on plasticity and its impact on the most widespread soil classification systems. Appl Clay Sci. 2018;161:57–63. https://doi.org/10.1016/j.clay.2018.04.011.
9. da Silva AMV, Delgado JMPQ, Guimarães AS, de Lima WMPB, Soares Gomez R, de Farias RP, de Lima ES, de Lima AGB. Industrial ceramic blocks for buildings: clay characterization and drying experimental study. Energies. 2020. https://doi.org/10.3390/en13112834.
10. Lapunova K, Bozhko YA, Lazareva YV, Orlova M, Kozlov G. Dynamic mineralogical and structural transformations in the process of siliceous opal clays firing. AIP Conf Proc. 2019. https://doi.org/10.1063/1.5138475.
11. Khoshnevis B, Bodiford M, Burks K, Ethridge E, Tucker D, Kim W, Toutanji H, Fiske M. Lunar contour crafting—a novel technique for ISRU-based habitat development. In: 43rd AIAA Aerospace Sciences Meeting and Exhibit. 2005. p. 538. https://doi.org/10.2514/6.2005-538.
12. Rasterhoff C. Mirroring two golden ages: values and visions in seventeenth-and nineteenth-century amsterdam. In: Van Damme I, De Munck Bert, Miles A, editors. Cities and creativity from the renaissance to the present. Milton Park: Routledge; 2017. p. 105–26.
13. Kashcheev ID, Zemlyanoi KG, Pavlova IA. The sintering of the ceramic materials based on the North-Onega bauxitized clay: Part 1. The granular composition effect. Nov Ogneup. 2018. https://doi.org/10.17073/1683-4518-2018-7-24-28.
14. Tang D, Hao L, Li Y, Li Z. Effect of clay functionally graded materials on dual gradient direct ink writing behavior and microstructure of geological model. Rapid Prototyp J. 2020;26(1):39–48. https://doi.org/10.1108/rpj-01-2019-0023.
15. Moses G, Etim RK, Sani JE, Nwude M. Desiccation-induced volumetric shrinkage characteristics of highly expansive tropical black clay treated with groundnut shell ash for barrier consideration. Civil Environ Res. 2019. https://doi.org/10.7176/cer/11-8-06.
16. Pavy S. A terracotta cooling device that integrates nature with modern technology. 2023. https://designwanted.com/biomimicry-cooler-nature-modern-technology/.

17. Sánchez-Soto PJ, Garzón E, Pérez-Villarejo L, Eliche-Quesada D. Sintering behaviour of a clay containing pyrophyllite, sericite and kaolinite as ceramic raw materials: looking for the optimum firing conditions. Bol de la Soc Esp de Cerám y Vidrio. 2023;62(1):26–39. https://doi.org/10.1016/j.bsecv.2021.09.001.
18. Chan SSL, Pennings RM, Edwards L, Franks GV. 3D printing of clay for decorative architectural applications: Effect of solids volume fraction on rheology and printability. Addit Manuf. 2020. https://doi.org/10.1016/j.addma.2020.101335.
19. Carr MM, Wang Y, Ghayoomi M, Newell P. Effects of 3D printing on clay permeability and strength. Transp Porous Media. 2023;148(3):499–518. https://doi.org/10.1007/s11242-023-01955-z.
20. Alonso Madrid J, Sotorrío Ortega G, Gorostiza Carabaño J, Olsson NOE, Tenorio Ríos JA. 3D claying: 3D printing and recycling clay. Crystals. 2023. https://doi.org/10.3390/cryst13030375.
21. Revelo CF, Colorado HA. 3D printing of kaolinite clay ceramics using the Direct Ink Writing (DIW) technique. Ceram Int. 2018;44(5):5673–82. https://doi.org/10.1016/j.ceramint.2017.12.219.
22. Marquez C, Mata JJ, Renteria A, Gonzalez D, Gomez SG, Lopez A, Baca AN, Nuñez A, Hassan MS, Burke V, Perlasca D, Wang Y, Xiong Y, Kruichak JN, Espalin D, Lin Y. Direct ink-write printing of ceramic clay with an embedded wireless temperature and relative humidity sensor. Sensors. 2023. https://doi.org/10.3390/s23063352.
23. Li H, Liu Y, Liu Y, Zeng Q, Hu K, Lu Z, Liang J. Effect of debinding temperature under an argon atmosphere on the microstructure and properties of 3D-printed alumina ceramics. Mater Charact. 2020. https://doi.org/10.1016/j.matchar.2020.110548.
24. Johanna L, Judith K, Alar J, Birgit M, Siim P. Material properties of clay and lime plaster for structural fire design. Fire Mater. 2019;45(3):355–65. https://doi.org/10.1002/fam.2798.
25. Wang C, Gong H, Wei W, Wu H, Luo X, Li N, Liang J, Khan SB, Xiao C, Lu B, Ma H, Long Y, Chen S. Vat photopolymerization of low-titanium lunar regolith simulant for optimal mechanical performance. Ceram Int. 2022;48(20):29752–62. https://doi.org/10.1016/j.ceramint.2022.06.235.
26. An D, Liu W, Xie Z, Li H, Luo X, Wu H, Huang M, Liang J, Tian Z, He R. A strategy for defects healing in 3D printed ceramic compact via cold isostatic pressing: sintering kinetic window and microstructure evolution. J Am Ceram Soc. 2019;102(5):2263–71. https://doi.org/10.1111/jace.16269.
27. Chen Z, Li J, Liu C, Liu Y, Zhu J, Lao C. Preparation of high solid loading and low viscosity ceramic slurries for photopolymerization-based 3D printing. Ceram Int. 2019;45(9):11549–57. https://doi.org/10.1016/j.ceramint.2019.03.024.
28. Chen Z, Liu C, Li J, Zhu J, Liu Y, Lao C, Feng J, Jiang M, Liu C, Wang P, Li Y. Mechanical properties and microstructures of 3D printed bulk cordierite parts. Ceram Int. 2019;45(15):19257–67. https://doi.org/10.1016/j.ceramint.2019.06.174.
29. Kim NP, Cho D, Zielewski M. Optimization of 3D printing parameters of Screw Type Extrusion (STE) for ceramics using the Taguchi method. Ceram Int. 2019;45(2):2351–60. https://doi.org/10.1016/j.ceramint.2018.10.152.
30. Zhang C, Luo Z, Liu C, Zhu J, Cao J, Yuan J, Wang P, Liu C, Lao C, Chen Z. Dimensional retention of photocured ceramic units during 3D printing and sintering processes. Ceram Int. 2021;47(8):11097–108. https://doi.org/10.1016/j.ceramint.2020.12.233.
31. Wiecinska P. Thermal degradation of organic additives used in colloidal shaping of ceramics investigated by the coupled DTA/TG/MS analysis. J Therm Anal Calorim. 2016;123(2):1419–30. https://doi.org/10.1007/s10973-015-5075-1.
32. Luz AP, Moreira MH, Braulio MAL, Parr C, Pandolfelli VC. Drying behavior of dense refractory ceramic castables: Part 1—General aspects and experimental techniques used to assess water removal. Ceram Int. 2021;47(16):22246–68. https://doi.org/10.1016/j.ceramint.2021.05.022.
33. de Lima AGB, Delgado JMPQ, Nascimento LPC, de Lima ES, de Oliveira VAB, Silva AMV, Silva JV. Clay ceramic materials: from fundamentals and manufacturing to drying process predictions. In: Delgado JMPQ, de Lima AGB, editors. Transport processes and separation technologies. Cham: Springer International Publishing; 2021. p. 1–29.
34. Mouiya M, Bouazizi A, Abourriche A, El Khessaimi Y, Benhammou A, El Hafiane Y, Taha Y, Oumam M, Abouliatim Y, Smith A, Hannache H. Effect of sintering temperature on the microstructure and mechanical behavior of porous ceramics made from clay and banana peel powder. Results Mater. 2019;4:100028. https://doi.org/10.1016/j.rinma.2019.100028.
35. Ji M, Xu J, Yu D, Chen M, El Mansori M. Influence of sintering temperatures on material properties and corresponding milling machinability of zirconia ceramics. J Manuf Process. 2021;68:646–56. https://doi.org/10.1016/j.jmapro.2021.05.012.
36. Niu SX, Luo YS, Li X, Chen YX, Cheng YZ, Dai SL, Zhang Q, Li H, Xu XQ. 3D printing of silica-based ceramic cores reinforced by alumina with controlled anisotropy. J Alloys Compd. 2022. https://doi.org/10.1016/j.jallcom.2022.166325.
37. Xiao C, Zheng K, Chen S, Li N, Shang X, Wang F, Liang J, Khan SB, Shen Y, Lu B, Ma H, Chen Z. Additive manufacturing of high solid content lunar regolith simulant paste based on vat photopolymerization and the effect of water addition on paste retention properties. Addit Manuf. 2023. https://doi.org/10.1016/j.addma.2023.103607.
38. Čelko L, Gutiérrez-Cano V, Casas-Luna M, Matula J, Oliver-Urrutia C, Remešová M, Dvořák K, Zikmund T, Kaiser J, Montufar EB. Characterization of porosity and hollow defects in ceramic objects built by extrusion additive manufacturing. Addit Manuf. 2021. https://doi.org/10.1016/j.addma.2021.102272.
39. Liu Z, Ma C, Chang Z, Yan P, Li F. Advances in crack formation mechanism and inhibition strategy for ceramic additive manufacturing. J Eur Ceram Soc. 2023;43(12):5078–98. https://doi.org/10.1016/j.jeurceramsoc.2023.05.008.
40. Chen W, Zou B, Huang C, Yang J, Li L, Liu J, Wang X. The defect detection of 3D-printed ceramic curved surface parts with low contrast based on deep learning. Ceram Int. 2023;49(2):2881–93. https://doi.org/10.1016/j.ceramint.2022.09.272.
41. Chen Z, Li Z, Li J, Liu C, Lao C, Fu Y, Liu C, Li Y, Wang P, He Y. 3D printing of ceramics: a review. J Eur Ceram Soc. 2019;39(4):661–87. https://doi.org/10.1016/j.jeurceramsoc.2018.11.013.
42. Balakrishnan HK, Dumée LF, Merenda A, Aubry C, Yuan D, Doeven EH, Guijt RM. 3D printing functionally graded porous materials for simultaneous fabrication of dense and porous structures in membrane-integrated fluidic devices. Small Struct. 2023. https://doi.org/10.1002/sstr.202200314.
43. Dutto A, Zanini M, Jeoffroy E, Tervoort E, Mhatre SA, Seibold ZB, Bechthold M, Studart AR. 3D printing of hierarchical porous ceramics for thermal insulation and evaporative cooling. Adv Mater Technol. 2022. https://doi.org/10.1002/admt.202201109.
44. Westman A. The capillary suction of some ceramic materials 1. J Am Ceram Soc. 1929;12(9):585–95. https://doi.org/10.1111/j.1151-2916.1929.tb18090.x.

45. Hambach M, Volkmer D. Properties of 3D-printed fiber-reinforced Portland cement paste. Cement Concr Compos. 2017;79:62–70. https://doi.org/10.1016/j.cemconcomp.2017.02.001.
46. Wang Q, Jia J, Zhao Y, Wu A. In situ measurement of full-field deformation for arc-based directed energy deposition via digital image correlation technology. Addit Manuf. 2023. https://doi.org/10.1016/j.addma.2023.103635.
47. Hanzlíček T, Perná I, Uličná K, Římal V, Štěpánková H. The evaluation of clay suitability for geopolymer technology. Minerals. 2020. https://doi.org/10.3390/min10100852.